LA-4440-TR

G. 3

LOS ALAMOS SCIENTIFIC LABORATORY
of the
University of California
LOS ALAMOS • NEW MEXICO

Numerical Experiments with a Nonlinear Chain

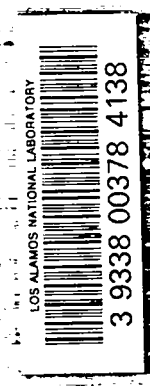

UNITED STATES
ATOMIC ENERGY COMMISSION
CONTRACT W-7405-ENG. 36

This translation has been prepared in response to a specific request; it is being given standard distribution because of its relevance to the nuclear energy program. Reasonable effort has been made to ensure accuracy but no guarantee is offered.

Printed in the United States of America. Available from
National Technical Information Service
U. S. Department of Commerce
Springfield, Virginia 22151
Price: Printed Copy $3.00; Microfiche $0.65

Distributed: November 1970

LA-4440-TR
UC-32, MATHEMATICS
AND COMPUTERS
TID-4500

LOS ALAMOS SCIENTIFIC LABORATORY
of the
University of California
LOS ALAMOS • NEW MEXICO

Numerical Experiments with a Nonlinear Chain

by

F. M. Izrailev
A. I. Khisamutdinov
B. V. Chirikov

Source: Preprint 252, Institute of Nuclear Physics, Novosibirsk, USSR Academy of Sciences, 1968.

Translated by

Helen J. Dahlby

NUMERICAL EXPERIMENTS WITH A NONLINEAR CHAIN

by

F. M. Izrailev, A. I. Khisamutdinov, and B. V. Chirikov

ABSTRACT

Results of numerical experiments with a chain of nonlinear coupled oscillators are presented. The experiment was to check the existence and position of the stochasticity border. Several methods to detect stochasticity were used, including energy spectrum, various correlations, and local instability. The results are in reasonable agreement with analytical estimates. They also demonstrate a very complex structure of the intermediate zone separating the region of stochasticity from that of Kolmogorov's stability. In particular the local instability begins at a considerably smaller β-value than one at which time correlations vanish. Even under the strongest excitation ($\beta = 1$, $E = 96$), the lowest modes haven't been completely stochastic. The fluctuations of the system's full energy, due to computational errors, were relatively large--up to 3%. Although the main parameters of the motion, such as local instability rate, haven't been affected by these errors, the trajectory itself had to be. Therefore further computation with higher accuracy and with a larger number of oscillators in the chain is desirable.

This work is a continuation of numerical experiments by Fermi, Pasta, and Ulam[1] to study the statistical properties of a chain of nonlinear coupled oscillators. The model chosen in Ref. 1 was convenient because it permits, in principle, any number of degrees of freedom and is relatively simple for numerical calculation (of course, with a limited number of degrees of freedom) and analytical estimates.

Furthermore, our test shows that this model is even much more convenient for numerical experiments (especially over a long time) than a first-order equation in partial derivatives of the Korteweg-DeVries type.[2] In the latter case, the calculating rate and operative memory of even the best contemporary electronic computers, such as the CDC-6600 or BESM-6 clearly is not sufficient. Of course, the situation can change considerably when the unique "Illiac-4," with 10^9 operations per second comes into use.[3]

The problem is interesting in that it throws light on the physical nature and the mechanism of appearance of statistical laws in the dynamic system. As Krylov[4] showed, this question is still open. The solution to this problem can be still more important in its practical applications. The emergence of statistical rules, or, for brevity, stochasticity, implies the development of the most dangerous instability of nonlinear fluctuations. On one hand, this instability develops rapidly enough, $\sim\sqrt{t}$, as any diffusion process; on the other hand, it covers a very wide range of values of parameters and initial conditions.

Even in 1955,[1] it was assumed that any nonlinearity always leads to stochasticity for a system with enough degrees of freedom. In particular,

this followed from Fermi's early work.[5] The evidence in Fermi's paper is unconvincing now, it seems, and Fermi himself doubted it and therefore decided to perform a verifying numerical experiment.[1] As is known, the experiment gave a negative result and showed the presence of a wide region of stability with almost-periodic movement.

Two other groups of experimental data indicate the presence of such a stable region. First, the motion of particles in accelerators, where there are always small nonlinear perturbations. Most significant in this respect are the data of Baconnier et al.[6] which established the stability of vibrations of protons about the equilibrium orbit during at least 10^9 vibration periods during which an additional nonlinear perturbation was specially introduced. On the other hand, the numerical experiments undertaken at CERN during planning for the synchrotron showed that with a nonlinear perturbation greater than some critical limit the emergence of some irregular instability is possible.[7] Apparently, this was the first indication of the existence of a stochasticity limit, dividing the stable and stochastic regions of nonlinear vibrations.

The other group of experimental data is related to the remarkable stability of the solar system. During $\sim 10^9$ vibration periods there are no signs of development of instability even if there are significant disruptions of the coplanarity and circular shape of the orbits. Of course, all these experiments, both "real" and calculated, can demonstrate stability for a finite time interval only. Stability for any time, or perpetual[8] stability, is proved analytically only for two degrees of freedom.[8,9] However, the invariance of an evenly dense system of tori revealed in these papers shows that if even for many degrees of freedom there is also instability,[10] leading finally to stochasticity (in formal accordance with the Fermi theorem[5]), the rate of development of this instability must be very slow, at least for most initial conditions. Therefore, even with many degrees of freedom it is natural to expect the presence of some stochasticity limit, beyond which rapid development of instability begins.

In its time, the result of Ref. 1 was very surprising, and evoked a series of theoretical papers[11-15] which attempted to explain the paradox that had arisen. In particular, Jackson[14] introduced a hypothesis of the existence of a stochasticity limit and gave a determination of its location. Our main problem is the numerical determination of the stochasticity limit for the simpler case of a cubic nonlinearity, which Jackson considered.

1. Calculation Scheme

We consider a chain of N - 1 oscillators (N = 32) interacting by a definite nonlinear rule. The equation of motion of each oscillator is

$$\ddot{x}_e = (x_{e+1} - 2x_e + x_{e-1}) + \beta\left[(x_{e+1} - x_e)^3 - (x_e - x_{e-1})^3\right] . \qquad (1)$$

The ends of the chain are rigidly secured: $x_0 = x_N = 0$. The coefficient β characterizes the magnitude of the nonlinear perturbation, and x_e is the displacement of the e-th oscillator from the equilibrium location.

Equation (1) belongs to the type $y'' = f(x,y)$, for which it is advantageous to use Scraton's proposed method[15] for numerical calculation. The advantage of this method compared to the Runge-Kutta method, for example, is that with the same accuracy the number of operations is significantly reduced. Let us present the equations of this algorithm for application to Eq. (1). We write Eq. (1) in the form

$$\ddot{x}_e = f(x_{e+1}, x_e, x_{e-1}) \qquad (2)$$

and introduce

$$F_e^{\xi} = h^2 \cdot f(x_{e+1}^{\xi}, x_e^{\xi}, x_{e-1}^{\xi}) ,$$

where h is the step in time and the index ξ denotes the time t at which the values of x are taken. Let us divide length h into three parts in the following proportions (if h is taken as unity):

$$\underline{0 \quad a \quad 1-a \quad 1} ,$$

where a is chosen as $a = \frac{5 - \sqrt{5}}{10} = 0.27639320$. We will subsequently omit the index e and show how to

obtain the values x^{n+1} and $\dot{x}^{n+1}$ at the moment of time n + 1, knowing x^n and $\dot{x}^n$. The time axis can be represented in the form

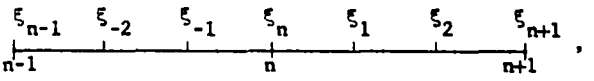

where $\xi_1 = n + ha$, $\xi_2 = n + h(1-a)$, $\xi_{-1} = n - ha$, $\xi_{-2} = n - h(1-a)$, and, correspondingly, $\xi_n = n$, $\xi_{n-1} = n - 1$, $\xi_{n+1} = n + 1$. Then x^{n+1} and $\dot{x}^{n+1}$ are determined by

$$x^{n+1} = x^n + h\dot{x}^n + \frac{1}{12} F^{\xi_n} + 0.30150283\ F^{\xi_1} + 0.11516383\ F^{\xi_2} + 0(h^7) \quad , \tag{3}$$

and

$$h\dot{x}^{n+1} = h\dot{x}^n + \frac{1}{12}\left(F^{\xi_n} + 5F^{\xi_1} + 5F^{\xi_2} + F^{\xi_{n+1}}\right) + 0(h^8).$$

The values of F^{ξ_1} and F^{ξ_2} can be found using

$$x^{\xi_1} = x^n + 0.27639320\ h\dot{x}^n + 0.06457768\ F^{\xi_n} - 0.03874353\ F^{\xi_{-1}} + 0.01871643\ F^{\xi_{-2}} - 0.00635398\ F^{\xi_{n-1}} + 0(h^6) \quad ;$$

and (4)

$$x^{\xi_2} = x^n + 0.72360680\ h\dot{x}^n + 0.29711983\ F^{\xi_1} - 0.12944272\ F^{\xi_n} + 0.10937164\ F^{\xi_{-1}} - 0.01574536\ F^{\xi_{-2}} + 0(h^6) \quad .$$

In addition, for the first step, knowledge of F^{-a}, F^{a-1}, and F^{-1} is necessary; we obtain x^{-a}, x^{a-1}, and x^{-1}, which correspond as follows.

$$x^{-1/2} = x^0 - 1/2\ h\dot{x}^0 + 1/8\ F^0 + 0(h^3) \quad ,$$

$$x^{-1} = x^0 - h\dot{x}^0 + 1/6\ (F^0 + 2F^{-1/2}) + 0(h^5) \quad ,$$

$$x^{-a} = x^0 - 0.27639320\ h\dot{x}^0 + 0.02861197\ F^0 + 0.01213107\ F^{-1/2} - 0.00254644\ F^{-1} + 0(h^5),$$

and (5)

$$x^{a-1} = x^0 - 0.72360680\ h\dot{x}^0 + 0.11805469\ F^0 + 0.16120227\ F^{-1/2} - 0.01745356\ F^{-1} + 0(h^5),$$

where x^0 and $\dot{x}^0$ are the initial values. Choice of the step h was dictated on the one hand by the smallness of the total energy fluctuations, which for Eq. (1) must be the constant of motion,

$$E = \frac{1}{2}\sum_{\ell=1}^{N-1}\left\{\dot{x}_e^2 + (x_{e+1} - x_e)^2\right\} + \frac{\beta}{4}\sum_{\ell=1}^{N-1}(x_{e+1} - x_e)^4 = \text{const} \quad , \tag{6}$$

and on the other hand by the possibility of tracing the behavior of the system over long times. In each case, it is indicated by E and $\Delta\dot{E}/E$. To ensure that the computing-scheme error does not affect the final result of the calculation, we conducted separate control tests with reduced h. Because the analytical calculations for the behavior of Eq. (1) are given in terms of normal (for the linear case, $\beta = 0$) coordinates (modes) of Q_k, over a certain number of steps, the conversion from x_e to Q_k is done according to

$$Q_k(t) = \sqrt{\frac{2}{N-1}}\sum_{\ell=1}^{N-1} x_e(t)\ \mathrm{Sin}\ \frac{\pi k\ell}{N} \quad , \tag{7}$$

and the energy of the modes is calculated,

$$E_k = \frac{\dot{Q}_k^2}{2} + \frac{\omega_k^2 Q_k^2}{2} \quad , \tag{8}$$

where ω_k is the linear frequency of the k-th mode:

$$\omega_k = 2\mathrm{Sin}\frac{\pi k}{2N} \quad . \tag{9}$$

As initial conditions, we gave the equal amplitudes of the modes $C_k^0 = C$, determined by

$$x_{max} = \frac{2(C^2)_m}{N-1} \quad , \tag{10}$$

where m is the number of excited modes and x_{max} (maximum displacement of the oscillator) is

assumed equal to unity. The initial velocities, $\dot{C}_k$, were always chosen as zero: $\dot{C}_k^0 = 0$. Then C_k and $\dot{C}_k$ were converted to x_e^0 and $\dot{x}_e^0$ by a conversion that is the converse of Eq. (7). We periodically printed out and interpreted all the values of interest.

2. Methods of Studying the Stochasticity

The main problem in analysis of numerical calculation results is the choice of a clear and convenient criterion that the movement is actually stochastic. We used the following methods in various cases.

1. Visual calculation by curves of the energy dependences of several modes on the time, as well as by the shape of the spectrum at different moments of time, $E_k(t)$. This method gives a clear enough result if at first only one mode is excited, as occurred in most cases in Ref. 1. An example of such a case for our calculations is given in Fig. 1 at the end of the report. The lower curve (δ) shows the clear almost-periodic energy fluctuations of the first mode. Unfortunately, such initial conditions are possible only for the very lowest modes. A mode $k \ll N$ can exchange energy directly only with the modes 3k, 5k, 7k, etc. In the case of excitation of a single sufficiently high mode, its energy remains practically unchanged. Figure 2 shows excitation of a single mode, K = 15. The small energy fluctuations are related to the interaction through the higher modes. (The reasons for the intensive energy exchange after $t \approx 5000$ are discussed below.) Therefore, we were forced to excite several modes at first. Figure 3 shows the time dependence of the energy of three modes (K = 16, 18, 19) with an initial excitation of five modes (K_0 = 14, 15, 16, 17, 18). It is seen that the energy exchange is fairly intricate because it is difficult to tell "by eye" whether a given motion is stochastic or not.

2. Change in the spectrum of fluctuations with time. Instead of observing the energy of some mode during a time t, one can determine the average energy value during the same time for each mode and find out how the energy concentrated at the initial moment t = 0 in certain modes was distributed. Such a redistribution of energy is shown in Fig. 4, which corresponds to the case of an initial excitation of three modes (K_0 = 28, 29, 30) (curve I). The other two curves (II and III) give the average (during the times t_1 and t_2) values of E_k. The averaging began at $t_0 = 5900$ in the calculation, which by this moment approaches a stationary exchange of energy between the modes; the values of $E_k(t)$ were chosen by Δt. It is seen that the energy was somehow redistributed, but only between adjacent modes; transfer of energy toward the higher modes ($N - K \ll N$) is easier than toward the lower modes ($K \ll N$). Also, we apparently observe an equilibrium state because the two curves (II and III) nearly coincide.

3. Time correlations were calculated for displacement of a certain oscillator, x_j, and for the energy of a certain mode of fluctuations, E_k, by

$$\rho(x_j, T) = \frac{\overline{x_j(t) \cdot x_j(t-T)}}{\overline{x_j^2(t)}} , \qquad (11)$$

and

$$\rho(E_k, T) = \frac{\overline{E_k(t)E_k(t-T)} - \overline{E_k(t)}^2}{\overline{E_k^2(t)} - \overline{E_k(t)}^2} . \qquad (12)$$

Here the line denotes averaging over t through equal intervals Δt, and T is the displacement with time. In all cases, in Eq. (11) j = 16, which for the chosen N = 32 corresponds to the middle oscillator of the chain.

The expected form of the correlation function can be visualized, taking for an example the Gaussian vibration spectrum:

$$f(\omega) = \frac{e^{\frac{-(\omega-\omega_0)^2}{2\delta^2}}}{\sqrt{2\pi}\,\delta} \qquad (13)$$

where δ is the width of the spectrum. The coefficient of the correlation is calculated directly and has the form:

$$\rho(t) = \frac{e^{\frac{-\omega_0^2}{\delta^2}} + \cos \omega_0 T}{1 + e^{-\omega_0^2/\delta^2}} \cdot e^{-\left(\frac{\delta T}{2}\right)^2} . \qquad (14)$$

For rapid vibrations, where $\omega_0 \gg \delta$, the correlation function is damping vibrations:

$$\rho(T) = e^{-\left(\frac{\delta T}{2}\right)^2} \cos \omega_0 T \quad . \qquad (15)$$

In the opposite limiting case, $\omega_0 \ll \delta$, we get a monotonic dependence (neglecting the small vibrations in the "tail"):

$$\rho(T) \approx e^{-\left(\frac{\delta T}{2}\right)^2} \quad , \qquad (16)$$

which is the amplitude curve for Eq. (15).

Figure 5 shows the time dependence of the modulus of the correlation coefficient. The irregular upper curve ($\omega_0 \gg \delta$) is partly explained by the large interval, ΔT ($> \omega_0^{-1}$), by which the values of the function $\rho(x_{16},T)$ were calculated. The lower curve (correlations of mode K = 15) corresponds, clearly, to the case $\omega_0 \sim \delta$. The asymmetry of the vibrations of $\rho(E_{15},T)$ relative to zero is clearly seen. The residual vibrations of $\rho(T)$ at large T, which are especially clear in Fig. 5a, can be completely explained by statistical errors in the calculation of $\Delta\rho$. These errors are not determined, of course, by the number of components in the averaging in Eqs. (11) and (12) because adjacent components are not independent. However, for a rough calculation one can simply assume that the sum in Eq. (12) is broken up into several independent parts, each of which includes the components inside the interval of correlation τ. Let us denote by the latter term the time interval during which the correlations are still significant. The value of τ is found from the correlation function itself. For example, in Fig. 3, $\tau \sim 100$. Because the dispersion of each of these parts is ~1, then, by the usual equation,

$$\Delta\rho \sim \sqrt{\tau/(t-T)} \quad , \qquad (17)$$

where t is the total time of the process, t - T determines the time during which the components in the calculation of ρ were accumulated. For Fig. 6, $\Delta\rho \sim 0.1$. The rapid damping of the correlation function, Eqs. (15) and (16) is characteristic for the continuous spectrum, which corresponds to our chosen stochastic movement, Eq. (13). In the case of almost-periodic movement, the correlation function can have the form of Eqs. (15) and (16), but only to a certain value of T, which is inversely proportional to the distance between the lines of the spectrum, after which it will be repeated. In other words, a quasi-period T_q appears for it. By numerical calculation, we can find only the lower limit of T_q. According to the data of Fig. 5, $T_q > 490$. To raise this limit, we calculated $\rho(E_k,T)$ and $\rho(x_{16},T)$ for values of T up to $T_0 = 4900$. For example, for the data of Fig. 4, the correlations have the form given in Fig. 6. The correlations substantially exceed the statistical fluctuations of $\Delta\rho$ and have a quasi-period. This is completely natural because the energy distribution in Fig. 4 shows that in this case even the highest modes lie at the stochasticity limit. In other cases, as in Figs. 10 and 13, the correlations are lacking within the limits of statistical error to T = 4900. The characteristic time of energy exchange between the modes is ~1000.

4. Correlations between modes were calculated by

$$\rho(E_k,E_{k'}) = \frac{\overline{E_k \cdot E_{k'}} - \bar{E}_k \cdot \bar{E}_{k'}}{\left|\left(\overline{E_k^2}-\bar{E}_k^2\right)\left(\overline{E_{k'}^2}-\bar{E}_k^2\right)\right|^{1/2}} \quad , \qquad (18)$$

where the values E_k and $E_{k'}$ are chosen at the same moment of time by Δt, and the line, as in Eqs. (11) and (12), denotes averaging over t. Because of the rule of conservation of the total energy of the system, the correlation coefficient of Eq. (18) differs from zero even for stochastic movement. It is easy to show that in the latter case it is equal to

$$\rho(E_k,E_{k'}) = -\frac{1}{\nu-1} \quad . \qquad (19)$$

Thus, knowledge of this coefficient affords the possibility of determining the effective (average) number of interacting modes. For example, for the case in Fig. 5, $\rho(E_{15},E_{17}) \approx -0.24 \pm 0.1$, from which $\nu \approx 5^{+2}_{-1}$. For the energy spectrum of the modes represented in Fig. 4, $\rho(E_{27},E_{28})$ gives $\nu \sim 8$, which generally corresponds to the number of modes between which all the energy was distributed. A rough calculation of the statistical error of $\rho(E_k,E_{k'})$ gives the value of $\Delta\rho$ (Eq. 17),

the same as for $p(E_k,T)$.

5. Local instability of the vibrations, which means that almost any trajectories which are close at first rapidly diverge exponentially in the process of movement. To study local instability, we used the property of spatial symmetry of our system, according to which even modes cannot appear in the process of movement if they were not excited at first.[1] Therefore, there is an exact solution, $E_{2k}(t) = 0$, and we were able to adequately trace the energy of the modes if a very small energy was imparted to them at first. We detected this unusual instability of the even modes accidentally. When we studied the excitation of a single mode, we found during calculation that the energy of the even ("forbidden") modes increases from machine zero ($\sim 10^{-19}$) to a significant value and becomes comparable to the energies of uneven modes. That is, from the very start there was an asymmetry in x_e^0 relative to the middle of the chain. The "culprit" turned out to be the procedure of calculating the sine, which enters into the conversion equation, which is the converse of Eq. (7). (Recall that, for initial conditions, Q_k^0 and $\dot{Q}_k^0$, and not x_e^0 and $\dot{x}_e^0$, were given). We discovered that the sine was calculated with a certain error, which depends on the number of the mode, as a result of which there also arose a weak asymmetry corresponding to some small excitation of even modes. Subsequently, when this was necessary, we carried out a special symmetrization of x_e^0 right after the transition from Q_k^0 and $\dot{Q}_k^0$ and x_e^0 and $\dot{x}_e^0$.

This effect has also been assumed because of the so-called method of local instability, which is generally the most effective method of determining that the system is in the stochasticity region, in view of the fact that the most characteristic property of stochasticity is local instability of motion. At the same time, in the stable region of the phase space, which corresponds to quasi-periodic motion, small disturbances fluctuate around some average value.

Figure 2b shows the case in which, because of rapidly developing instability, the energy earlier concentrated in one mode ($K_0 = 15$) suddenly passes into the adjacent modes. Figure 2a gives the logarithmic time dependence of the energy of the individual modes, by which one can calculate the rate of instability development. This method permitted detecting the weak instability for $K_0 = 1$ also. The parameters are taken from Ref. 1, whose authors considered the motion in this case to be quasi-periodic. Actually, Fig. 1 does not give rise to doubt about this. Nonetheless, Fig. 1a shows that an instability, although weak, exists, and can affect the overall behavior (for example, of the first mode) after a long enough time. In Fig. 7, the growth of even modes ($K_0 = 15,17$) is once more demonstrated; it is noticeable that the far ($K = 2,30$) modes "grow" later than the closer ($K = 14, 18$) ones, although the growth rate is approximately the same for all. Note that the transfer of energy to the highest modes ($K = 30$) occurs more rapidly than that to the lowest ($K = 2$) ones. This effect was noted in Ref. 1.

By this method, giving at some moment of time ($t_0 = 75$) an initial disturbance of the even modes ($\sim 10^{-14}E$), we studied the stochasticity limit. For this, the odd modes were excited in threes, and the energy growth rate of the adjacent even modes was determined. Figure 8 gives the characteristic dependences of the energy of the even modes on the time; using these one can, albeit with some error, determine the dependence of the rate of development of the instability on the nonlinearity parameter, β.

The method is extremely convenient because of its use of visual methods and because it does not require a long calculating time. Further, a single calculation immediately gives the distance between two close trajectories. Nonetheless, to be convinced that such a choice of trajectories was not special, we conducted two experiments. The first consisted in exciting three uneven modes ($K_0 = 27, 29,31$) at first, but we carried out symmetrization; i.e., we held the energies of the even modes rigidly equal to zero for the whole time, and miscalculated two variants with differing Q_k^0 ($\delta Q_k^0 \approx 10^{-8}$). Then we determined the acceleration rate of these two trajectories. In the second case, we excited both even and odd modes as well ($m = 3$, $K_0 = 28,29,30$) and compared two close trajectories analogously. In all cases (for sufficiently large β) we observed an exponential acceleration of the trajectories, indicating local instability of

motion.

3. Basic Results

As already mentioned, our main problem was the experimental determination of the stochasticity limit for a chain of nonlinear oscillators. The analytical calculation for this limit, obtained by Jackson,[14] has the form:

$$3\beta_{crit}\frac{E}{N-1}\sim\begin{cases}\frac{\sqrt{m}}{K}; & K\ll N\\ 10\frac{m}{N^2}\left(\frac{K}{N}\right)^2; & N-K\ll N\end{cases}, \qquad (20)$$

where E is the total energy of Eq. (1) and m is the number of excited modes. The shape of the border is shown in Fig. 14 (straight lines, $m \sim 1$).

Experimental determination of the stochasticity limit was made by the method of local instability (Sec. 2). The combined data are given in Fig. 15 in the form of vertical lengths giving the range of values of the rate of growth, $1/\tau$ (cf. Fig. 8). The groups of data, I, II, III, IV, were obtained by the growth of even modes with an initial excitation of three adjacent odd modes in different parts of the spectrum. Groups V and VI were obtained by the acceleration of close trajectories. In the first case (V), the same modes were excited as for (I), but with symmetrization, i.e., with total elimination of even modes. In the second case (VI) both even and odd modes (K_0 = 28,29,30) were excited.

In Fig. 15, a semilogarithmic scale was used, in accordance with the expected dependence,[16]

$$\frac{1}{\tau} = \Omega \ln \beta/\beta_{crit}, \qquad (21)$$

where β_{crit} lies at the stochasticity limit, Eq. (20), and Ω is of the order of the distance between resonances.[14] Actually, for large β the experimental data lie on straight lines within the error limit. However, for small β there are significant deviations. We do not know for sure the cause of these deviations. We can only introduce two different hypotheses for their explanation.

The first of these links the deviations, always on the side of large $1/\tau$, with other, denser resonance systems. This leads simultaneously to decrease in β_{crit}, which is determined by the intersection of the interpolation line in Fig. 15 with the axis of abscissae, and to decrease in the slope of the line. Qualitatively, this is also observed in Fig. 15. This effect is seen especially clearly in the excitation of lower modes, where besides the "basic" line (I) it is possible to draw with confidence a second line (IV). In other cases, the effect is less evident.

A quantitative comparison can be made by measuring the slope of the interpolation lines in Fig. 15. The average value of this slope for all the groups besides (IV) gives $\langle\Omega\rangle \approx 2.6\cdot10^{-2}$, which more or less agrees with the expected calculation $\Omega \sim \pi/N \approx 0.1$. For line IV: $\Omega \approx 10^{-3}$. This can be compared with that predicted by the theory of a dense system of resonances $\Omega \sim (\pi/N)^3 \approx 10^{-3}$. The theory also predicts that in this case β_{crit} ($\sim\Omega$) must decrease by as many times again. This is actually confirmed in order of magnitude:

$$\Omega(III)/\Omega(IV) = 25;\ \beta_{crit}(III)/\beta_{crit}(IV) \approx 37.$$

The question arises of the difference, in such a case, in the two stochasticity limits from the point of view of the behavior of the system as a whole. The answer is that the denser system of resonances can be, and in the given case actually is, not wide enough. Therefore, overlap of the resonances of such a system generally does not lead to complete stochasticity; instead, a more or less narrow stochastic band with limited change in the energy of the interacting modes is formed.

Apparently, this effect explains the behavior of the system for the case, represented in Fig. 2, which is strange at first glance. Thus, the upper curve in this figure clearly indicates local instability of the motion. However, this instability apparently is not appreciably developed because it does not appear at all on the lower curve. In particular, the successive maxima in Fig. 2b differ from each other by several percent; however, this difference does not increase exponentially, as in Fig. 2a.

There arises the still more important question of whether such a stochastic layer can lead to a significant redistribution of energy between the modes after a sufficiently long time. Although we have no experimental data on this, we know that, generally speaking, it is possible. It is possible

owing to the so-called Arnold diffusion, the mechanism of which is related to the crossing of different stochastic layers of a multidimensional system.[10] However, this instability develops extremely slowly,[10,17] and therefore it is sensible to consider it separately from the strong instability caused by overlap of a wide (and less dense) system of resonances. The term "strong" here means that the whole disturbance, which is proportional to β, Eq. (1), behaves as "accidental," without any additional small multiplier whatever. Just such a stochasticity limit is represented in Fig. 14.

Comparison of this stochasticity with three experimental points shows that the dependence of β_{crit} on K corresponds to that expected; however, the absolute value is about three times smaller. Such a difference cannot be considered very serious, in view of the roughness of the calculation of Eq. (20).[2] This roughness is associated not only with the indefinite numerical multiplier in Eq. (20), but also with the small number of excited modes. The latter effect is demonstrated by lines V and VI in Fig. 15. Thus, for line V β_{crit} is approximately twice as large as for line I; the only difference between them is the total absence of even modes for V. A still more significant difference occurs in the case of excitation of modes of mixed parity (VI), where β_{crit} exceeds the value for the comparable case of (I) by almost an order. It is difficult to say why this is so. It could be, for example, the decrease in the number of modes of the same parity. In any case, this demonstrates once more the very complex structure of the transition zone, but, at the same time, shows the coincidence in order of magnitude of the expected and experimental location of the stochasticity limit.

Let us return to the deviation of the experimental data from the lines in Fig. 15. A completely different explanation for this phenomenon is possible, which is that the dependence of $1/\tau$ on β_{crit} is not logarithmic, Eq. (21). It is possible, for example, to approximate this dependence by a power function. For this, we plot the same experimental data in a double logarithmic scale (Fig. 16). Unfortunately, they also fit within the limit of errors on the straight lines. Thus, at present, the experimental errors are too large; to distinguish between the two hypotheses, further numerical experiments with greater accuracy are necessary.

Analytical calculations, to be published later, show that, depending on the phase relations between the resonances, another dependence of $\tau^{-1}(\beta_{crit})$ is actually possible, namely,

$$\tau^{-1} \sim \Omega\left(\frac{\beta}{\beta_{crit}}\right)^{4/3} . \qquad (22)$$

From this, in particular, it follows that the slope of the interpolation lines in a double logarithmic scale must be $n = 4/3 \approx 1.33$. The experimental values of the slope are given as subscripts in Fig. 16; the average value (except for III) is: $\langle n \rangle = 1.28$. All the values except for III coincide with the expected value (4/3) within the limits of experimental error. In the case of (III), both the slope of the interpolation line and the overall grouping of the experimental points differ considerably from the calculation, Eq. (22). This indicates, apparently, that at least in this case the dependence, Eq. (21), occurs.

The stochasticity limit in Fig. 16 corresponds to the vertical asymptote of the dependence $\tau^{-1}(\beta)$. Although the experimental data in Fig. 16 also do not exclude such a possibility, a quantitative determination of β_{crit} does not seem possible owing to the large errors. Therefore we were obliged, perhaps without complete justification, to use the data of Fig. 15 for this goal.

We have already seen that local instability does not necessarily mean strong stochasticity (although, apparently, it necessarily leads to real instability). Therefore it is desirable to use other methods to be convinced that for sufficiently large β and E our Eq. (1) is actually stochastic. Three controls of the calculation were performed in the limiting time possible under our conditions $t_{max} \sim 10^4$.

In the first case three odd modes ($K_0 = 15$, 17,19) were excited, as for case (II) in Fig. 15, but with symmetrization. The value $\beta \approx 0.0314$ was chosen approximately twice as large as β_{crit} in Fig. 15. The correlations of the 15th mode and the displacement of the central oscillator were measured, as well as the correlations between modes 15 and 17. The results are given in Fig. 11. It is seen that the correlations have an almost-periodic nature, and the number of interacting

modes remains practically unchanged: $N_{int.} = 4 \pm 1$.

This result does not necessarily contradict the data on the location of the stochasticity limit in Fig. 15. First, if the system is close to the stochasticity limit, the energy cannot be spread over a large number of modes, since this increases m and stops the stochasticity, Eq. (20). Second, the conditions for the onset of stochasticity are actually determined by the energy of the interacting modes,[14] and not just by the total energy, as is assumed for simplicity in Eq. (20). But in such a case the energy of each mode cannot decrease significantly near the stochasticity limit, because, again, the conditions of stochasticity are disrupted. This means that only partial exchange of energy between modes is possible, which, in turn, leads to residual correlations. However, if we take $\beta \gg \beta_{crit}$, we must already obtain "genuine" stochasticity.

The second control calculation corresponds also to $\beta/\beta_{crit} \approx 28$ (Fig. 13). Here the energy is actually distributed among almost all the modes, excluding only the very lowest, for which fulfillment of the criterion for stochasticity, Eq. (20), is difficult. It is easy to calculate the critical value of K to which the stochasticity reaches:

$$K_{crit} \sim K_0 \frac{m}{m_0} \cdot \frac{\beta_{crit}}{\beta} \sim 2 \quad ,$$

where we assume: $K_0 = 17$, $m_0 = 3$, $m \approx N = 32$. This result is also confirmed by the value of $\rho(E_{15}, E_{17})$ (Fig. 13). Because of large experimental errors, it is possible to calculate only the lower limit for the number of interacting modes: $N_{int.} \geqslant 8$. From the data of Fig. 13, we also see that within the limits of statistical error (± 0.1) correlations of the 15th mode are lacking. Correlations with x are related mainly to the fact that the stochasticity does not reach to the first mode. Note that the correlations die out slowly. It is possible that this is somehow related to the effect of the calculation errors (see below), but, if so, why do they not die out in Fig. 11? Another possible explanation is that the motion of the first mode, which is responsible for the correlation with x, is nevertheless stochastic, but after a significantly greater time, because this mode lies in the transition zone (Fig. 12).

Finally, in the last control calculation, all the modes were excited with an equal amplitude and, consequently, substantially different energy (Fig. 9, curve I). If the calculation of Eq. (20) is expanded in this case also, then the critical value of K will be $K_{crit} \sim N\sqrt{m}/3\beta E \sim 1/2$, where we used the data of Fig. 9, $\beta = 1$, $E = 96$, $m \approx N = 32$. The result shows that the lowest modes lie practically at the stochasticity limit and therefore can show some anomalies. This actually occurs, according to the picture of the energy distribution (Fig. 9, curve III) and the correlations with x (Fig. 10a). At the same time, correlations of the 13th mode are again lacking within the limits of statistical error, and correlations between the modes lead to the value $N_{int.} \geqslant 7$.

In summing up, we can state that all the experimental data confirm Jackson's hypothesis[14] on the presence of a stochasticity limit for Eq. (1) and, moreover, confirm , in order of magnitude, the calculation, Eq. (20), of the location of this limit. Our weakest point is the significant calculation error, which was controlled as regards change in the total energy of the system (see subscripts to figures); in the absence of errors, $\Delta E \equiv 0$. This especially concerns the three control experiments (Figs. 9 to 13) where $\Delta E/E$ reaches 3%. Can these errors by themselves cause stochasticity? We think not. A confirmation of this is the significant residual correlations (Fig. 11) and the absence of energy exchange (Fig. 12) for small β. Another control of the effect of errors was carried out for an experiment with local instability. With decrease of the step by a factor of 2, $\Delta E/E$ decreased from 3 to 0.03%; thus exponential growth curves of the type given in Fig. 8 changed somewhat; however, the value of the parameter of interest, $1/\tau$, remained the same as before within the limits of experimental error.

Nonetheless, continuation of numerical experiments with a more accurate nonlinear chain and a larger number of oscillators seems useful.

We thank A. Chistiakov for help in carrying out the calculations and E. Krushkal' for useful critical observations.

REFERENCES

1. E. Fermi, J. Pasta, and S. Ulam, "Studies of Nonlinear Problems I," Los Alamos Scientific Laboratory report LA-1940, 1955.
2. N. J. Zabusky and M. D. Kruskal, Phys. Rev. Lett. 15, 240 (1965).
3. W. B. Riley, Electronics 40, 141 (1967).
4. N. S. Krylov, "Raboty po Obosnovaniiu Statisticheskoi Fiziki" (Work on the Basis of Statistical Physics), Publishing House of the Academy of Sciences, USSR, 1950.
5. E. Fermi, Phys. Zeitschr. 24, 261 (1923).
6. Y. Baconnier, B. de Raad, and Ch. Steinbach, "Experiments on Beam Survival and Nonlinear Resonances," in the CERN PS, Proc. Vth Intern. Conf. on High Energy Accelerators, Frascati, 1955.
7. F. K. Goward, in Lectures on the Theory and Design of an Alternating-Gradient Proton Synchrotron presented by Members of the CERN Protron Synchrotron Group at the Conference on the Alternating-Gradient Proton Synchrotron held at the Institute of Physics of the University of Geneva, Geneva, Switzerland, October 26-28, 1953, NP-5070; M. G. N. Hine, ibid.
8. V. I. Arnol'd, Uspekhi Matematicheskikh Nauk 18, 91 (1963).
9. A. N. Kolmogorov, Dokl. Akad. Nauk 98, 527 (1954).
10. V. I. Arnol'd, Dokl. Akad. Nauk 156, 9 (1964).
11. M. D. Kruskal and N. J. Zabusky, J. Math. Phys. 5, 231 (1964).
12. J. Ford, J. Math. Phys. 2, 387 (1961); J. Ford and J. Waters, J. Math. Phys. 4, 1293 (1963).
13. E. A. Jackson, J. Math. Phys. 4, 551, 686 (1963).
14. E. M. Izrailev and B. V. Chirikov, Dokl. Akad. Nauk 166, 57 (1966).
15. R. E. Scraton, Computer Journal 6, 386 (1964).
16. B. V. Chirikov, "Kogda Dinamicheskaia Sistema Stanovitsia Statisticheskoi?" (When Does a Dynamic System Become Statistical?) Preprint at Intern. Congress of Mathematicians, Moscow, 1966.
17. B. Chirikov, E. Keil, and A. Sessler, "The Stochasticity Limit of Many-Dimensional Non-Linear Oscillating Systems," CERN Report, to be published.

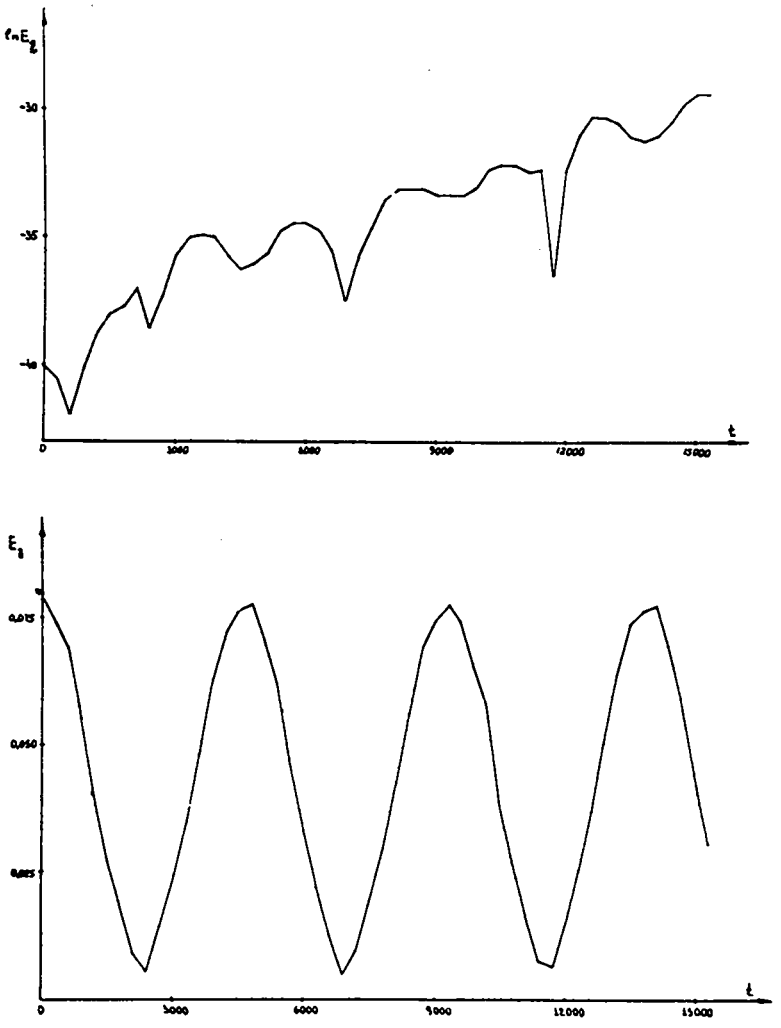

Fig. 1. First mode and small second mode excited at the beginning ($E_1^0 \approx 0.0788$; $E_2^0 \approx 5.3 \cdot 10^{-18}$). Above - logarithmic dependence of second mode energy; below - first mode energy; $h = 1/2$; $\beta = 8$; $t_{max} \approx 15{,}3000$; $\Delta E/E \approx 0.15\%$.

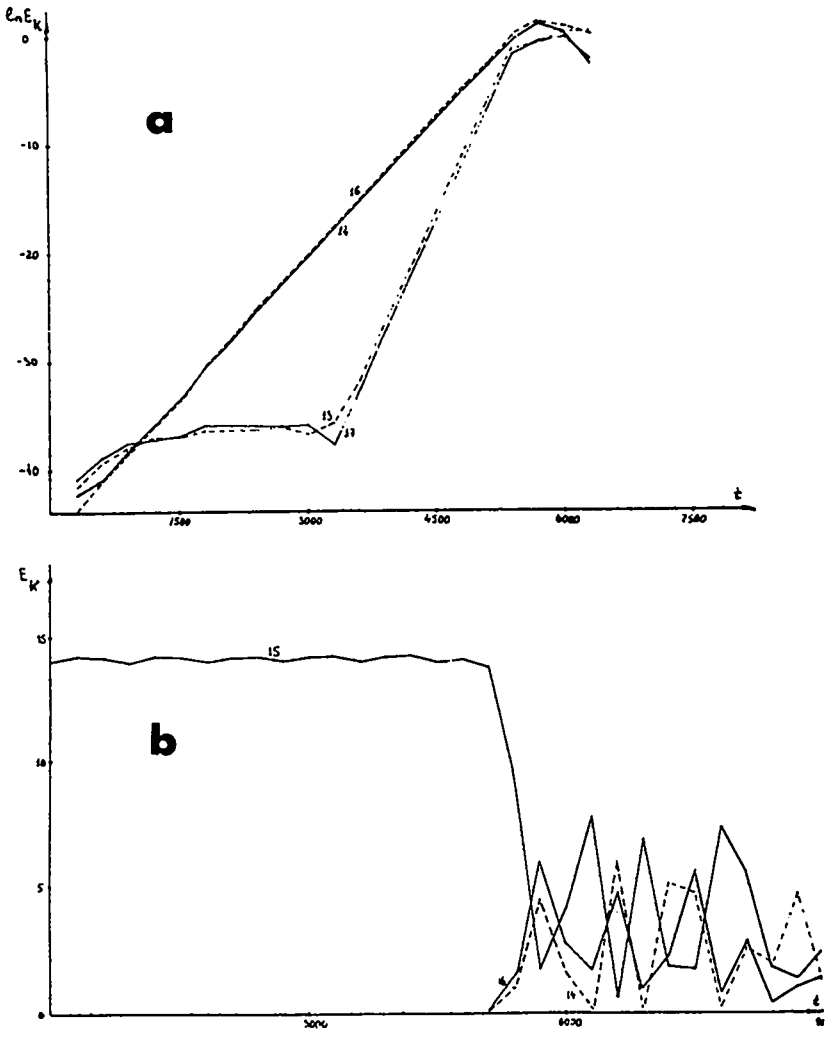

Fig. 2. Initial excitation of single 15th mode; a - logarithmic energy growth of several modes, b - dependence of energies of modes (K = 14,15,16) on time; figures indicate number of mode; h ≈ 1/6; β ≈ 0.0314; t_{max} ≈ 9000; E ≈ 14.1; ΔE/E ≈ 1.5%.

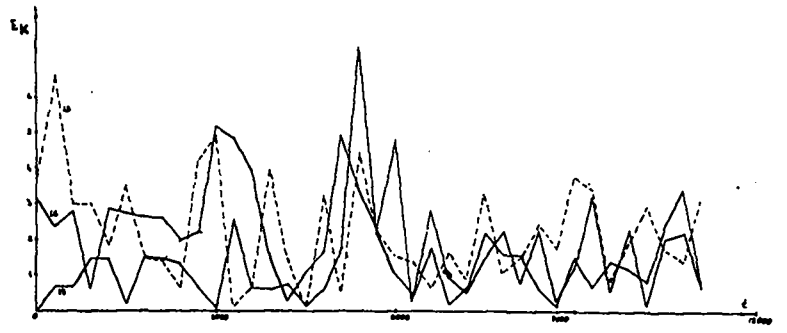

Fig. 3. Excited group of five modes (K_0 = 14,15,16,17,18; m = 5). The time dependence of the energies of modes with the numbers K = 16, 18, 19 is given; h ≈ 1/3; β ≈ 0.0314; t_{max} ≈ 11,100; E ≈ 16.1; ΔE/E ≈ 1.5%.

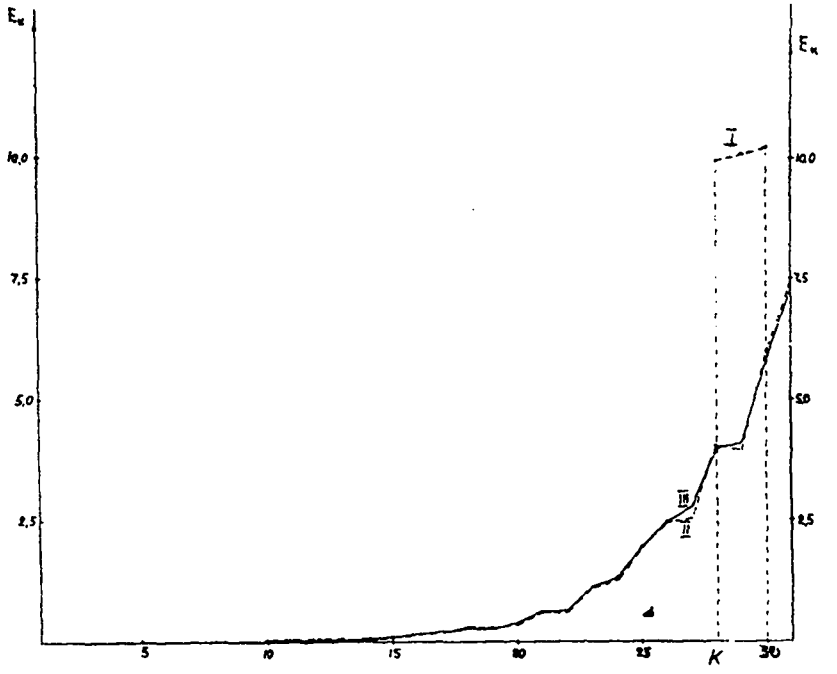

Fig. 4. Energy spectrum for initial excitation of three highest modes (K_0 = 28,29,30; m = 3, curve I).
Curve II gives the average energies of each mode at the moment t_1 ≈ 9300; III - at the moment t_2 ≈ 10,500; h ≈ 1/6; β ≈ 0.06; Δt = 1; E ≈ 35.2; ΔE/E ≈ 4.3%.

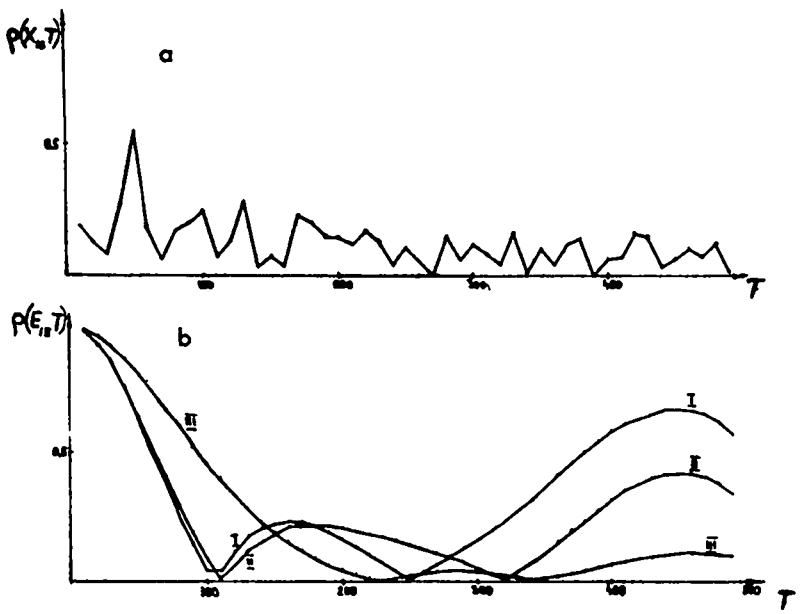

Fig. 5. Correlations of displacement of oscillator (a) and of energy of 15th mode (b) for case of Fig. 3. Curve I corresponds to a calculation time $t_1 \approx 3150$; curve II - $t_2 \approx 4500$; curve III - $t_3 \approx 11{,}100$; $\Delta T = 10$; $\Delta t = 1$; $\rho(E_{13}, E_{15}) \approx -(0.24 \pm 0.10)$ (for t_3).

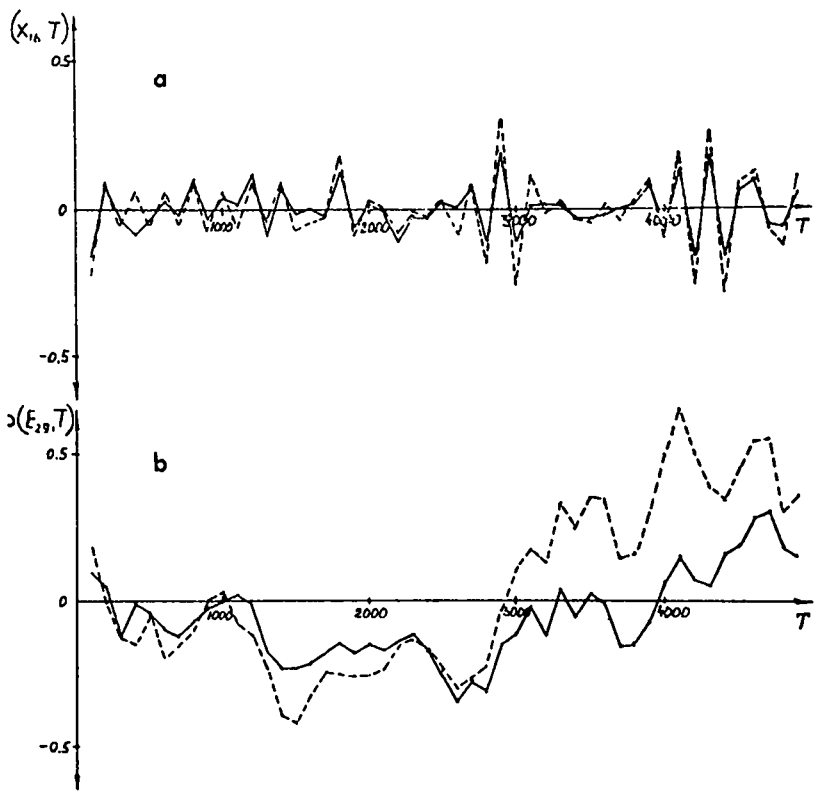

Fig. 6. Correlations of displacement of the oscillator (a) and of the energy of the 29th mode (b) for the case of Fig. 4. The broken lines correspond to a calculation time $t_1 \approx 9300$; the solid lines - $t_2 \approx 10{,}500$; $\Delta T = 100$; $\Delta t = 1$; $\rho(E_{27}, E_{29}) \approx -(0.15 \pm 0.10)$ (for t_2).

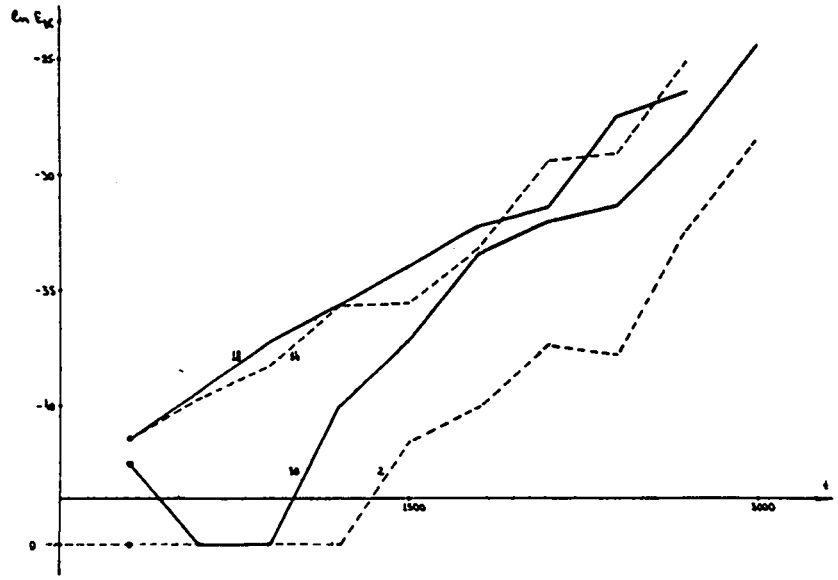

Fig. 7. Logarithmic growth of even modes for initial excitation of odd modes (K_0 = 15,17; m = 2).
Figures indicate number of modes; zero on the graph is machine zero, corresponding to $E_x \sim 10^{-20}$; h ≈ 1/6; β ≈ 0.0314; t_{max} ≈ 3000; E ≈ 20; ΔE/E ≈ 3.5%.

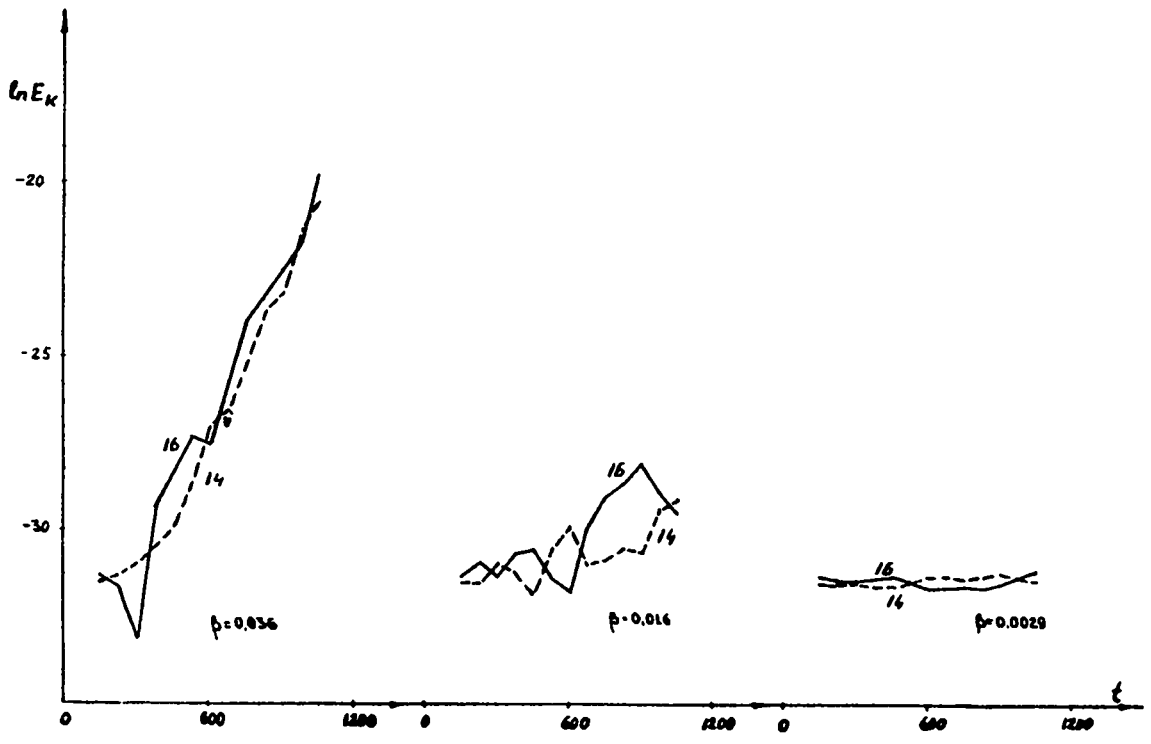

Fig. 8. Characteristic behavior of even modes (K = 14,16) for different values of the parameter β; K_0 = 15,17,19; m = 3; h ≈ 1/3; t_{max} ≈ 1050; E ≈ 17; $(\Delta E/E)_{max}$ ≈ 0.2%.

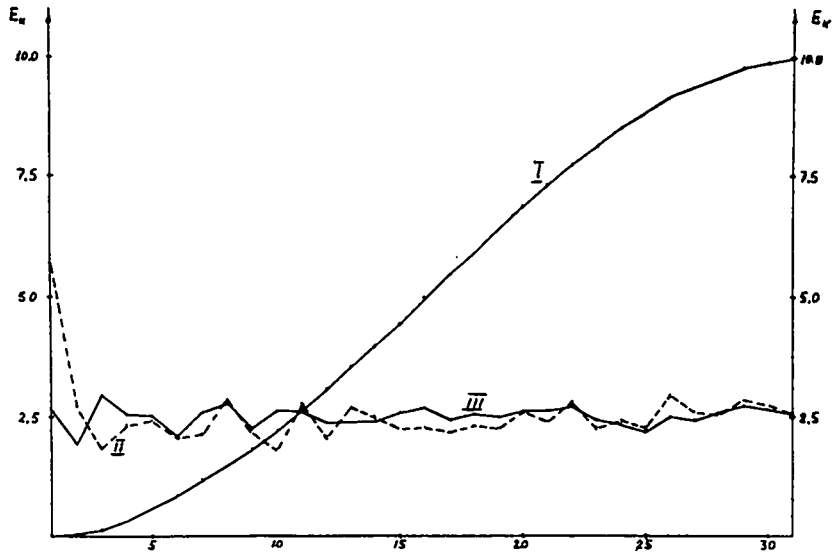

Fig. 9. Energy spectrum for initial excitation of all modes (curve I); curve II- energy spectrum of modes for time of calculation $t_1 \approx 6750$; curve III - for $t_2 \approx 11{,}025$; $h \approx 1/12$; $\beta = 1.0$; $\Delta t = 1$; $E \approx 96$; $\Delta E/E \approx 2.4\%$.

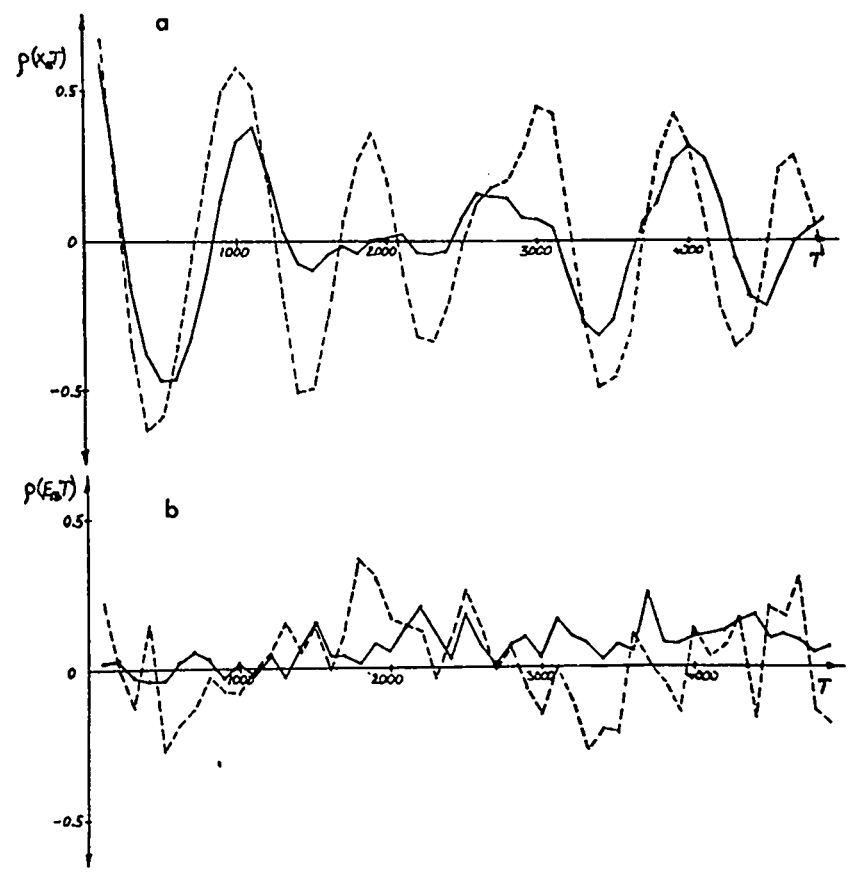

Fig. 10. Correlations for data of Fig. 9; broken lines correspond to calculation time t_1, solid lines to time t_2; $\Delta T = 100$; $\Delta t = 1$; $\rho(E_{13}, E_{15}) \approx -(0 \text{ to } 0.14)$ (for t_2).

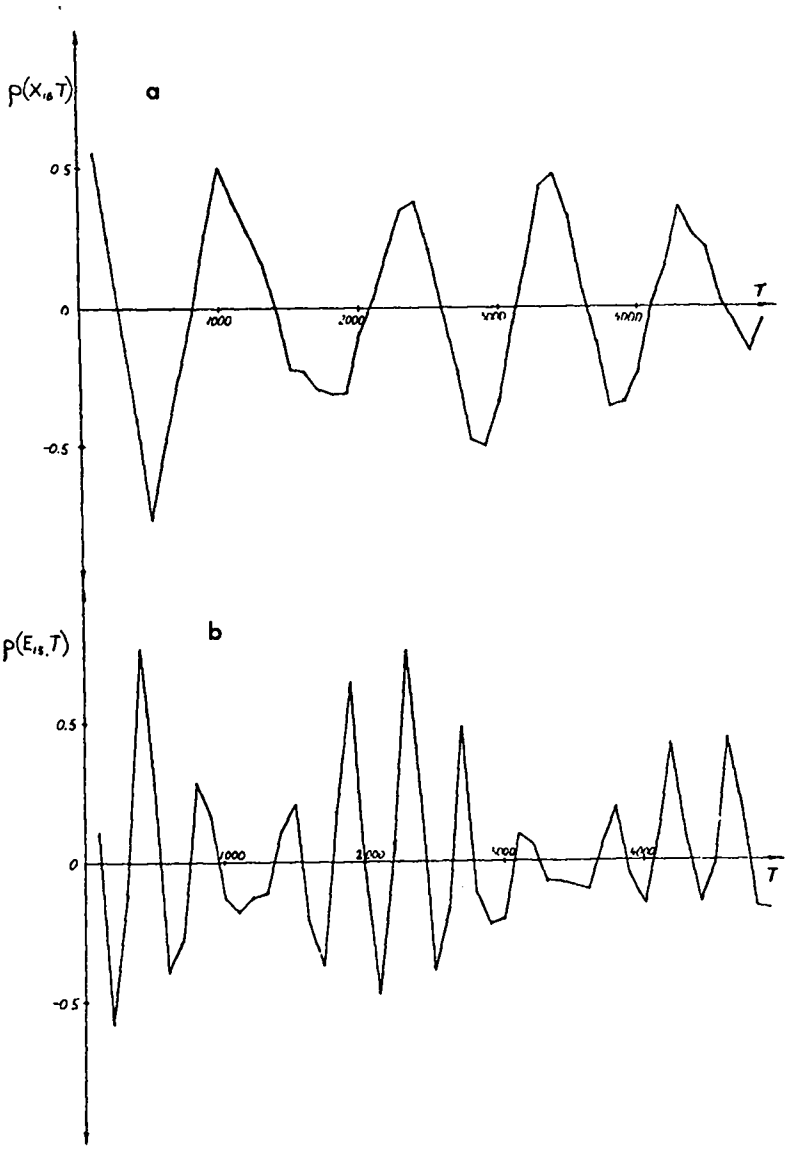

Fig. 11. Correlations for initial excitation of three odd modes (K_0 = 15,17,19; m = 3) with symmetrization; h ≈ 1/3; β ≈ 0.0314; t_{max} ≈ 18,300; ΔT = 100; Δt = 1; E ≈ 17; ΔE/E ≈ 3%; $\rho(E_{15},E_{17}) \approx -(0.30 \pm 0.07)$.

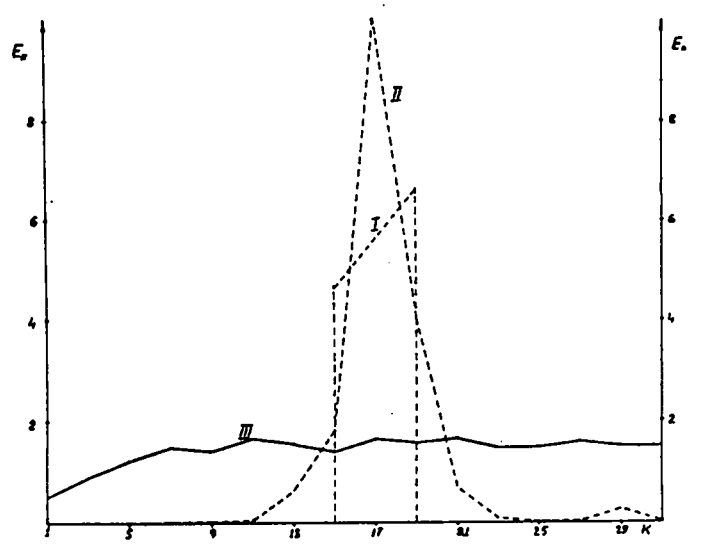

Fig. 12. Energy spectrum for initial excitation of three modes (K = 15,17,19; m = 3) with symmetrization (curve I); curve II corresponds to the average energies of the modes for the data of Fig. 11; curve III - for the data of Fig. 13.

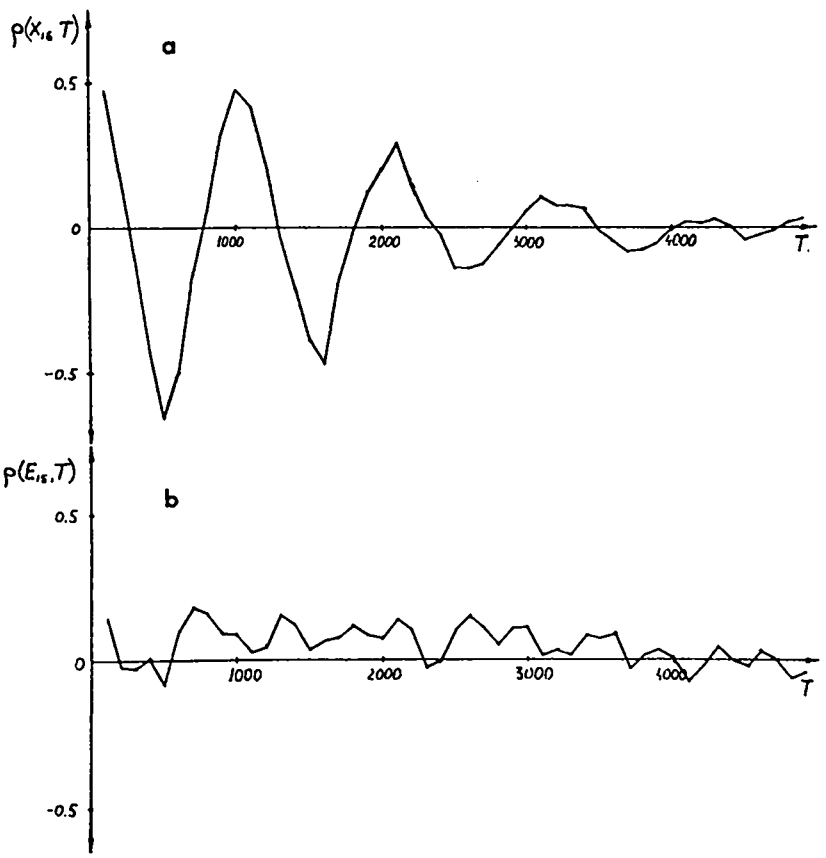

Fig. 13. Correlations for initial excitation of three odd modes (K_0 = 15,17,19; m = 3) with symmetrization; h ≈ 1/6; β ≈ 0.314; t_{max} ≈ 16,050; ΔT = 100; Δt = 1; E ≈ 24; ΔE/E ≈ 2%; $\rho(E_{15},E_{17})$ = ~(0 to 0.13).

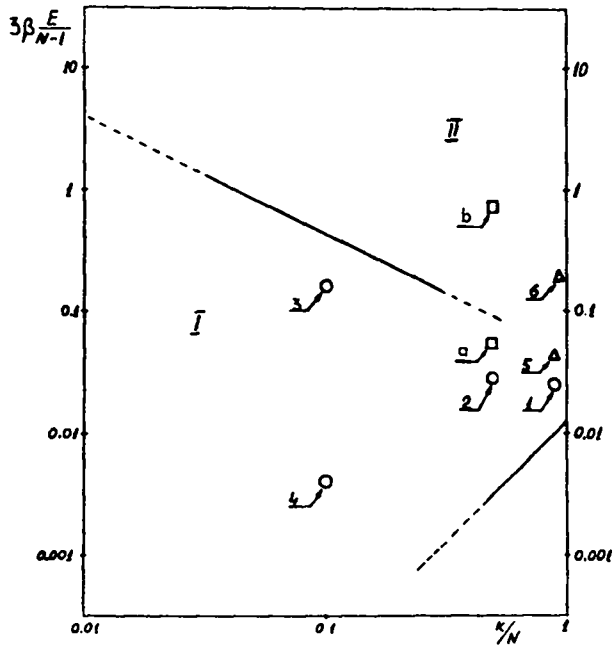

Fig. 14. Shape of stochasticity limit from the criterion of Eq. (20) (straight lines) and summary of experimental results:
I - Kolmogorov stability region;
II - stochasticity region.
Points 1, 2, 3, 4, 5, and 6 correspond to β_{crit} obtained from lines I, II, III, IV, V, and VI, given in Fig. 15; point a corresponds to the data of Fig. 11; point b to the data of Fig. 13.

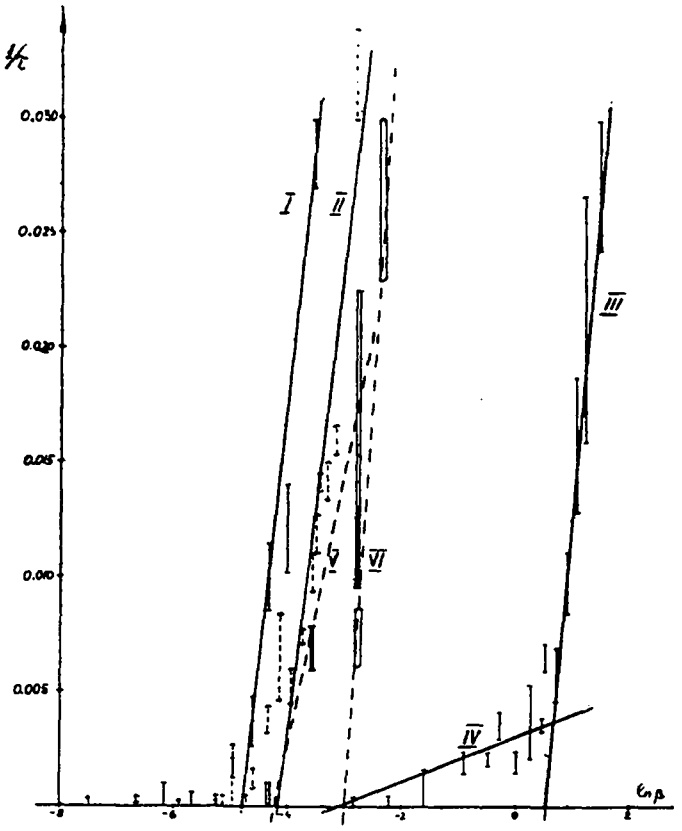

Fig. 15. Dependence of rate of local instability development on parameter β. Initial conditions: K_0 = 27,29,31 (I), E ≈ 30; K_0 = 15,17,19 (II), E ≈ 17; K_0 = 1,3,5 (III) and (IV), E ≈ 0.95; K_0 = 27,29,31 with symmetrization (V), E ≈ 30; K_0 = 28,29,30 (VI); E ≈ 35. The straight lines approximate the dependence, Eq. (21), and permit determining β_{crit}. Values of $1/\tau$ are given with experimental errors. For I: $\beta_{crit} \approx 8.7 \cdot 10^{-3}$, $\Omega \approx 2.4 \cdot 10^{-2}$; for II: $\beta_{crit} \approx 1.6 \cdot 10^{-2}$, $\Omega \approx 2.2 \cdot 10^{-2}$; for III: $\beta_{crit} \approx 1.7 \cdot 10^{-2}$, $\Omega \approx 2.9 \cdot 10^{-2}$; for IV: $\beta_{crit} \approx 4.6 \cdot 10^{-2}$, $\Omega \approx 1.0 \cdot 10^{-3}$; for V: $\beta_{crit} \approx 1.6 \cdot 10^{-2}$, $\Omega \approx 1.3 \cdot 10^{-2}$; for VI: $\beta_{crit} \approx 5 \cdot 10^{-2}$, $\Omega \approx 4.0 \cdot 10^{-2}$.

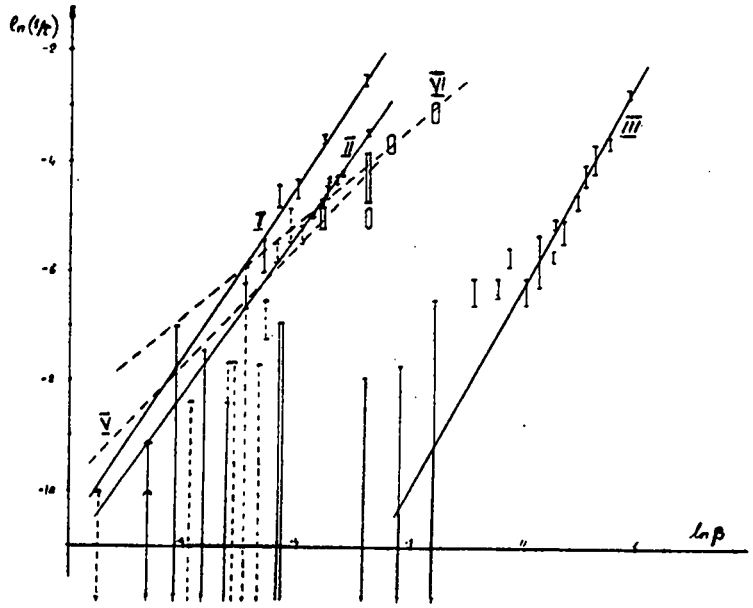

Fig. 16. The same as Fig. 15, but with a double logarithmic scale. The straight lines approximate the dependence, Eq. (22). The arrows show that within the limits of experimental error $1/\tau = 0$ is possible; for I- $n = 1.6 \pm 0.3$; for II- $n = 1.5 \pm 0.2$; for III- $n = 1.9 \pm 0.2$; for V- $n = 1.1 \pm 0.5$; for VI- $n = 0.9 \pm 0.4$.